Magnetic and Ionospheric Observations in the Far Eastern Region of Russia During the Magnetic Storm of 5 April 2010

Baishev D.G.[1], Moiseyev A.V.[1], Boroyev R.N.[1], Kobyakova S.E.[1], Stepanov A.E.[1], Mandrikova O.V.[2,3,4], Solovev I.S.[2,3,4], Khomutov S.Yu.[2], Polozov Yu.A.[2], Yoshikawa A.[5], Yumoto K.[5]

[1]Yu.G.Shafer Institute of Cosmophysical Research and Aeronomy SB RAS, Yakutsk, Russia
[2]Institute of Cosmophysical Research and Radiowave Propagation FEB RAS, Paratunka, Russia
[3]Kamchatka State Technical University, Petropavlovsk-Kamchatsky, Russia
[4]Saint Petersburg Electrotechnical University "LETI", Saint Petersburg, Russia
[5]International Center for Space Weather Science and Education, Kyushu University, Fukuoka, Japan

E mail (baishev@ikfia.sbras.ru).

Accepted: 30 September 2015

Abstract. Magnetic and ionospheric disturbances in the far eastern region of Russia during the magnetic storm of 5 April 2010 are studied using data of geophysical stations operated by IKFIA SB RAS and IKIR FEB RAS. By performing wavelet analysis of experimental data, the wavelet powers of geomagnetic perturbations at different stations are estimated, in an attempt to investigate the dynamical development of a geomagnetic storm. It is shown that, though weak geomagnetic disturbances were present prior to the main phase of magnetic storm, the variations of the magnetic field during a storm development were found to be rather strong. The highest intensity of geomagnetic disturbances during the interplanetary shock at the Earth's magnetosphere was observed at KTN (L~9) while at ZYK (L~4) strongest geomagnetic perturbations occurred during the magnetospheric substorm with the onset at 09:03 UT. Large geomagnetic fluctuations were recorded at TIX and CHD (L~5-6), when the High-Intensity Long-Duration Continuous AE Activity (HILDCAA) was observed on 6 April 2010. Ionospheric conditions at YAK (L~3.4) and PET (L~2.2) were characterized by a pre-storm enhancement in the electron density in the F2 layer on 4 April 2010 and prolonged negative phase of the ionospheric storm during the main and recovery phases of magnetic storm on 6-8 April 2010. These experimental results underscore the importance of multi-instrumental observations and provide clues to the complex interactive processes.

Keywords: magnetic storm, magnetic and ionospheric disturbances, magnetometer, digisonde, wavelet transformation

Introduction

The response of the ionospheric F layer to magnetic storms, commonly called ionospheric storms, is known to be very complex (e.g., Buonsanto, 1999; Mendillo, 2006 and references therein). It consists of positive and negative phases, the understanding of which is very challenging in space and in time. The morphological features of ionospheric storms and the main processes controlling their behavior have been described in a series of review articles (Prolls, 1995; Rees, 1995; Buonsanto, 1999; Danilov, 2001; Danilov and Laštovička, 2001; Mendillo, 2006). Despite extensive efforts in observations, theory, and numerical modeling, comprehensive understanding and accurate descriptions of ionospheric response to magnetic storms is far from complete.

The magnetic storm on 5 April 2010 with its beginning at 08:26 UT was caused by a coronal mass ejection which was unleashed from the Sun on 3 April 2010, and arrived at the Earth two days later (Möstl et al, 2010). Despite being a relatively weak storm (the minimum Dst was about -50 nT on 5 April) it nevertheless had some devastating space weather impacts, including the malfunction of the Galaxy 15 communication satellite (Allen, 2010).

Mandricova et al. (2014) performed a detailed analysis of the geomagnetic disturbances during magnetic storm and strong magnetospheric substorm on 5 April 2010 using data from magnetic stations of the far eastern region of Russia using in-house developed algorithms. By selected components of perturbed variations of the magnetic field they defined the time of occurrence and the periods of most intense geomagnetic disturbances. Based on the wavelet technique, spatial-temporal pattern of magnetic disturbance development in the region of interest was studied by them. Mandrikova et al. (2014b) analyzed only the cosmic ray data along with the geomagnetic data in their study. In the present study using ionospheric data from Paratunka and Yakutsk along with magnetic data from the far eastern region of Russia, before and during the magnetic storm of 5 April 2010, the intensity of ionospheric disturbances along with the abnormal periods were estimated using wavelet transforms.

Special attention has been paid to a development of sudden storm commencement and global substorm

in the interval of 07:00-10:00 UT on 5 April 2010 and pre-storm enhancement of critical frequency foF2 at ionospheric stations Yakutsk and Paratunka on 4 April 2010.

Materials and methods

We used the interplanetary magnetic field (IMF) and solar wind from the ACE Science Center, http://www.srl.caltech.edu/ACE/ASC, and magnetic data from observatories of institutes IKIR FEB RAS and IKFIA SB RAS (see Table 1 and Figure 1).

Three-component fluxgate magnetometers MAGDAS (Yumoto et al., 2006; Baishev et al., 2013) with a sensitivity up to 0.01 nT and sampling of 10 Hz were installed under Agreements between ICSWSE, Kyushu University, Japan, and our institutes, including the MAGDAS COLD model (PET, MGD, CPS) and MAGDAS-9 model (KTN, TIX, ZGN, YAK, CHD, ZYK). Both one-second and one-minute values of horizontal component H of the geomagnetic field were used for wavelet analysis.

Ionospheric data at observatory PET were from an upgraded old Russain Ionosonde with a digital receiver and computer operation. The peak power of the radiated pulse had been ~2 kW, the frequency range is about 1-15 MHz.

The Digisonde Portable Sounder DPS (Reinisch et al., 1997) is the system with a low power transmitter (300 W) employing intrapulse phase coding, digital pulse compression and Doppler integration and the four crossed magnetic dipole receiving antennas produced by the University of Massachusetts Lowell's Center for Atmospheric Research (UMLCAR, http://ulcar.uml.edu/).

On the basis of *the wavelet packet* decomposition, geomagnetic field variation can be represented as (Mandrikova et al., 2013, 2014b):

$$f_0(t) = \sum_n c_{-m,n}\varphi_{-m,n}(t) + \sum_{j\in I}\sum_n d_{j,n}\Psi_{j,n}(t) + \sum_{j\notin I}\sum_n d_{j,n}\Psi_{j,n}(t) = f_{trend}(t) + f_{dist}(t) + e(t), \quad (1)$$

Table 1. List of stations used in analysis. The corrected geomagnetic coordinates (CGM) were calculated for the epoch 2010.0 at an altitude of 110 km using the algorithm based on the DGRF/IGRF geomagnetic field models at http://omniweb.gsfc.nasa.gov/vitmo/cgm_vitmo.html.

Station	Code	Geodetic coordinates		corr.geomagnetic coordinates		L-parameter
		latitude	longitude	latitude	longitude	
Kotelny	KTN	76.0	137.9	70.7	202.7	9.3
Tixie	TIX	71.6	128.8	66.3	198.2	6.3
Chokurdakh	CHD	70.6	147.9	65.3	213.8	5.8
Zhigansk	ZGN	66.8	123.4	61.7	195.1	4.5
Zyryanka	ZYK	65.8	150.8	60.3	218.3	4.1
Yakutsk	YAK	62.0	129.8	56.6	201.8	3.4
Magadan	MGD	59.6	150.8	53.6	220.2	2.9
Paratunka	PET	52.9	158.3	46.6	227.4	2.2
Khabarovsk	KHB	47.6	134.7	41.5	207.6	1.8

where $f_{trend}(t) = \sum_n c_{-6,n}\varphi_{-6,n}(t)$ describes the undisturbed level of the horizontal component of the Earth magnetic field during quiet period, and $f_{dist}(t) = \sum_{j\in I} g_j(t)$, where $g_j(t) = \sum_n d_{j,n}\Psi_{j,n}(t)$ describes geomagnetic perturbations. Component $e(t) = \sum_{j\notin I}\sum_n d_{j,n}\Psi_{j,n}(t)$ represents the noise. I is a set of indices of the disturbed components.

The measure of geomagnetic perturbation component $g_j(t)$ on the scale j is determined as $A_j = \max_n\left(\left|d_{j,n}\right|\right)$ (Mandrikova et al., 2013, 2014b).

To estimate a power of geomagnetic perturbations the continuous wavelet transform (Daubechies 1992; Chui 1992) determined as

$$W_\Psi f_{b,a} := |a|^{-1/2}\int_{-\infty}^{\infty} f(t)\Psi\left(\frac{t-b}{a}\right)dt,$$

$f \in L^2(R), a, b \in R, a \neq 0.$ has been used

A power of geomagnetic perturbations at the moment $t=b$ on analyzed scale a is estimated as

$$e_{b,a} = \left|W_\Psi f_{b,a}\right| \quad (2)$$

A power of field perturbations at the time moment $t = b$ is

$$E_b = \sum_a e_{b,a} \quad (3)$$

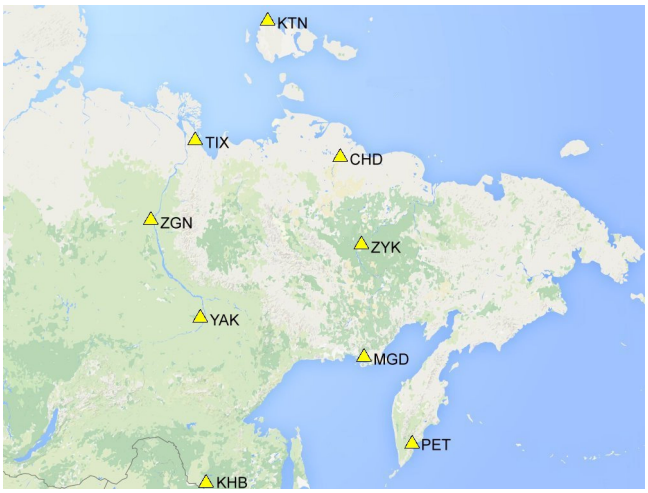

Figure 1: Location of magnetic stations in the far eastern region of Russia using Google map service.

Selection of anomalies in the ionosphere was based on continuous wavelet transformation and thresholding functions:

$$P_{T_a}(W_\Psi f_{b,a}) = \begin{cases} W_\Psi f_{b,a}, если \left| W_\Psi f_{b,a} - W_\Psi f_{b,a}^{med} \right| \geq T_a \\ 0, если \left| W_\Psi f_{b,a} - W_\Psi f_{b,a}^{med} \right| < T_a \end{cases}, \quad (4)$$

where threshold $T_a = U * St_a$ determines a presence of anomalies on the scale a near the point ξ, contained in the carrier $\Psi_{b,a}$, U is threshold coefficient, $St_a = \sqrt{\frac{1}{\Phi - 1}\sum_{k=1}^{\Phi}\left(W_\Psi f_{b,a} - \overline{W_\Psi f_{b,a}}\right)^2}$, $\overline{W_\Psi f_{b,a}}$ и $W_\Psi f_{b,a}^{med}$ are mean square deviation, mean value and median of critical frequency, determined separately for each hour in a sliding time window of length Φ.

To estimate the threshold coefficient U we used a posteriori risk (Levin, 1963). Determination of the ionosphere status was performed according to ionograms which also was correlated with geomagnetic data (using geomagnetic K index). *A power of ionospheric anomalies* at a time moment $t = b$ was estimated as

$$I_b = \sum_a \left| P_{T_a}(W_\Psi f_{b,a}) \right| \quad (5)$$

Data Analysis

Near-Earth environment

On 5 April 2010 an interplanetary (IP) shock was detected by the Wind spacecraft ahead of Earth, followed by a fast (average speed 650 km/s) interplanetary coronal mass ejection (ICME). During the subsequent moderate magnetic storm (minimum Dst =-72 nT, maximum Kp=8-), communication with the Galaxy 15 satellite was lost (Möstl et al., 2010).

Figure 2 shows the in situ observations by Wind SWE (Ogilvie et al., 1995) and MFI (Lepping et al., 1995). The first solid line from left is the shock arrival on 5 April 2010, 07:58 UT. The second and third solid lines indicate the magnetic cloud interval, from 5 April, 12:05 UT, to 6 April, 13:20 UT. From profile of IMF Bz it is evident that a strong (minimum = −15 nT) and short interval of negative IMF Bz in the sheath coincided with the storm commencement. In the ICME back region, too, it is the negative IMF Bz which is responsible for prolonging the storm growth phase. In between these two regions, when IMF Bz ≥ 0 nT, it is the large, negative IMF which accounts for the continued ring current intensity. Maximum Kp=8- was registered during sheath event while minimum Dst =-72 nT was occurred after magnetic cloud event on 6 April 2010.

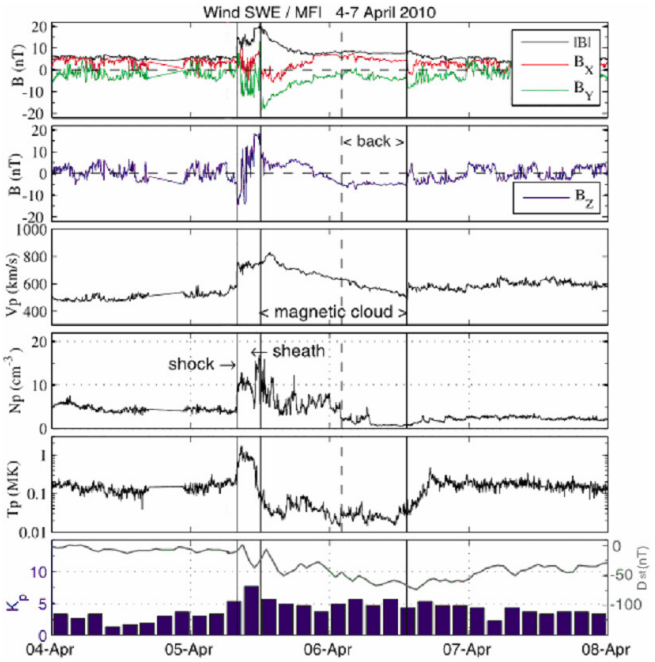

Figure 2: Interplanetary magnetic field and solar wind plasma data from the Wind spacecraft observations (Möstl et al., 2011). From top to bottom: magnetic field magnitude and components in GSE coordinates, proton bulk velocity, proton number density, proton temperature, planetary geomagnetic indices: Dst (black line, hourly) and Kp (blue bars, every 3 hours). The first vertical solid line from left is the shock arrival. Second and third solid lines indicate the magnetic cloud interval.

Geomagnetic field

Figure 3 presents the one-minute variations of the horizontal component H of the geomagnetic field recorded at stations in the far eastern region of Russia on 3-7 April 2010. At the beginning of the storm (~08:26 UT on 5 April 2010), a sharp increase of geomagnetic field disturbances was observed at stations from high to middle latitudes (stations KTN, ZYK, YAK and PET). The geomagnetic variations during a storm evolution were dynamic and were followed by a series of intense fluctuations during the period of 5-7 April 2010 as the ICME passed across the Earth. The highest geomagnetic disturbance during the interplanetary shock at the Earth's magnetosphere was recorded at

KTN (L~9). When the High-Intensity Long-Duration Continuous AE Activity (HILDCAA) was observed on April 6 2010, during the time when large geomagnetic fluctuations were recorded at TIX and CHD (L~5-6). At subauroral (ZYK) and middle (YAK, PET) latitudes large geomagnetic disturbance as spike was occurred during a magnetospheric substorm with the onset at 09:03 UT on 5 April 2010 (Kleimenova et al., 2013).

The results of the estimation of geomagnetic perturbation power (see eq. (3)) at Figure 4 show a similar behavior of geomagnetic disturbances over the far eastern region of Russia. An increase of geomagnetic perturbations was seen at ~08:15 UT on 5 April 2010. During the initial phase of magnetic storm, the strongest wavelet power of magnetic disturbance was observed in the interval of 08:43-09:34 UT (stations KTN, ZYK, YAK and PET). Large increase in geomagnetic activity was noticed in the night MLT hours during the global substorm with its onset at 09:03 UT (Kleimenova et al., 2013), when THEMIS AL was less than -2000 nT (Connors et al., 2011). Note that large magnetic intensities at TIX and CHD were seen during HILDCAA event on 6 April 2010

For more detailed picture, we processed one-second magnetic data (Figure 5) and investigated in detail the time interval of the sudden storm commencement (SSC) and global substorm from 07:00 UT till 10:00 UT. The wavelet spectra of selected perturbed component in the magnetic field variations $f_{dist}(t)$ (see eq. (1)) presented in Figure 5 shows a detailed space-time pattern before and during the event at all the stations considered.

All the stations were in the evening sector (see Table 1), and the positive variations of geomagnetic field H-component (eastward electrojet) was marked

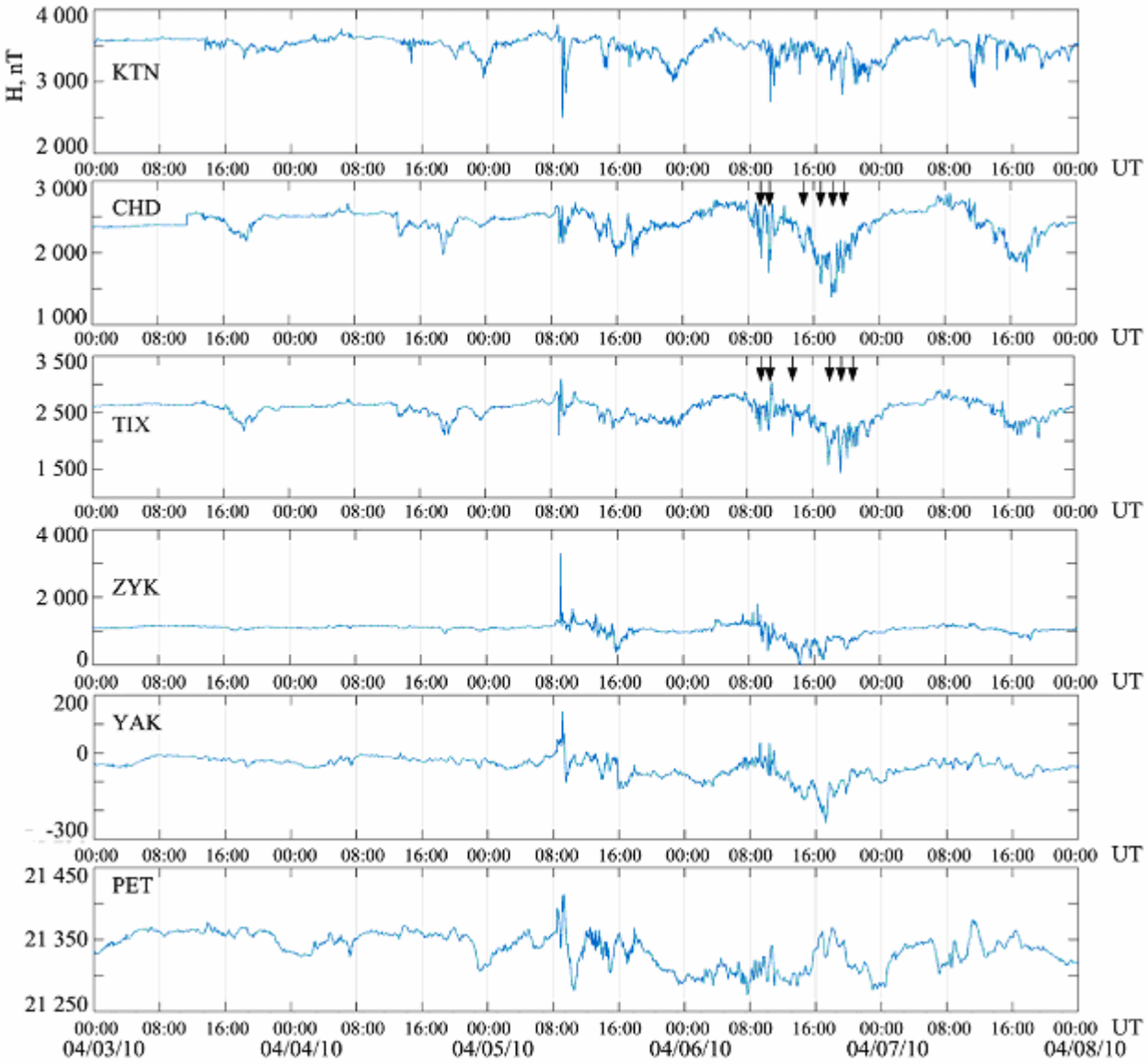

Figure 3: Variation of the geomagnetic field H-component with 1-min resolution at stations in the far eastern region of Russia on 3-7 April 2010. Large geomagnetic fluctuations at CHD and KTN during HILDCAA event marked by vertical arrows.

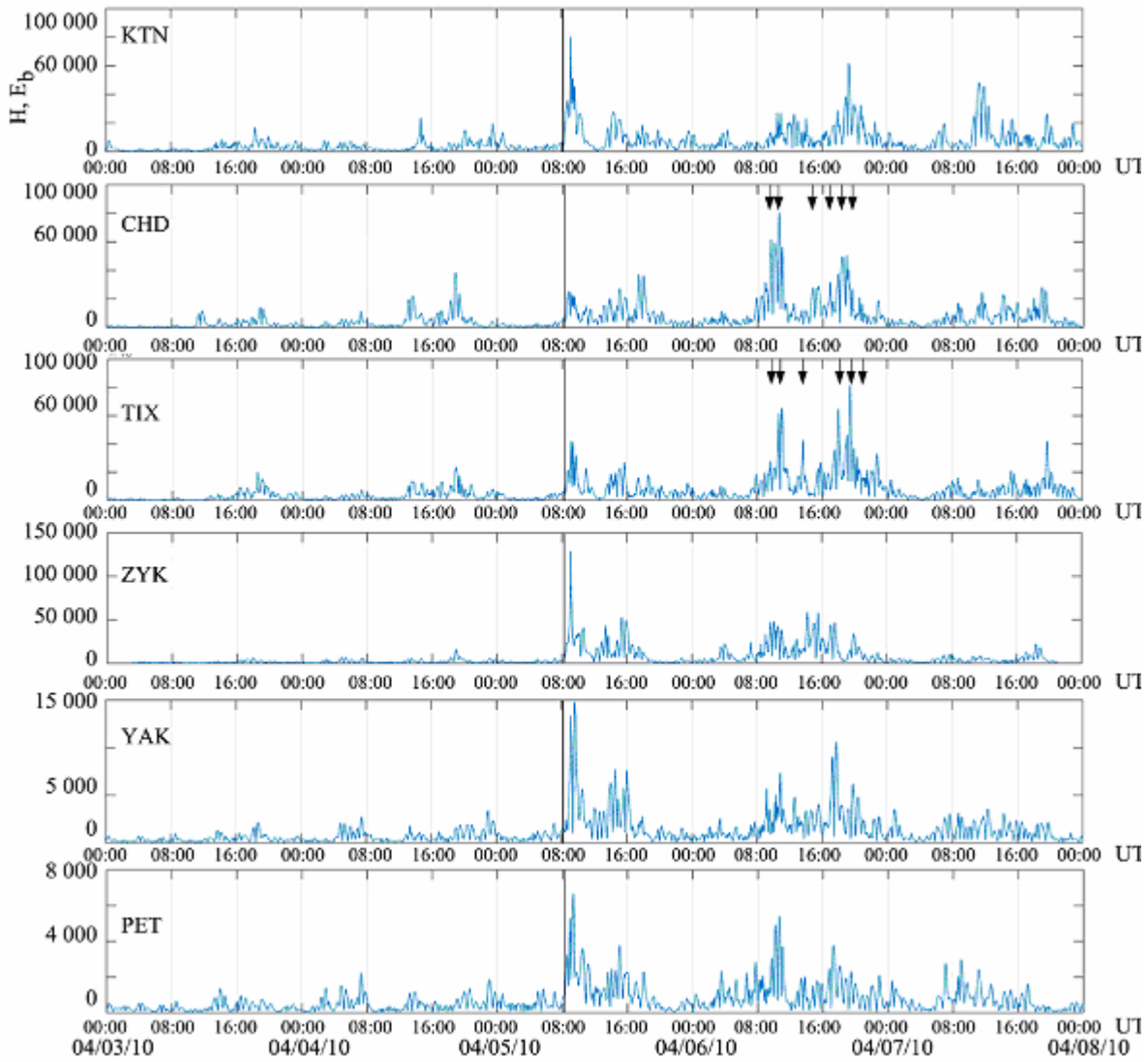

Figure 4: Estimation of a power of geomagnetic perturbations on 3-7 April 2010 (in according to eq. (3)). The vertical solid line indicate a moment of increase of geomagnetic perturbations. Large geomagnetic fluctuations at CHD and KTN during HILDCAA event marked by vertical arrows.

by red and the negative (westward electrojet) was marked by blue. At all stations, before the magnetic storm, an expansion and shift of wavelet power spectrum towards the high frequency range occurred, which indicate of the growth of geomagnetic activity. At high-latitude stations KTN, CHD, TIX positive and negative perturbations have a general character and a spectrum convergence is observed up to the magnetospheric substorm onset. At ZYK strongest geomagnetic perturbations occurred during the magnetospheric substorm clearly distinguishing the three active phase of perturbations. On the other hand, at mid-latitudes (MGD, PET, KHB) an active phase from 08:20 to 08:40 UT with a largest perturbations in the band of 35-60 minutes coinciding the SSC is highlighted. After the beginning of the storm, at about 09:30 UT a narrowing and shift of the spectrum to the low-frequency range, which characterizes a decrease of geomagnetic activity, could be observed.

Ionosphere

It is known that a sharp fluctuations in ionospheric electron density (ionospheric storm) can be in negative phase (negative ionospheric storm) with lower density, and in positive phase (positive ionospheric storm) with higher density. Additional energy inputs in the polar region and the consequent temperature increase/thermal expansion are capable of changing the altitude distribution of neutral constituents of the atmosphere with a net increase in the concentration of N2 relative to O. The temperature rises at ionospheric altitudes, resulting in a larger ionospheric recombination coefficient, and thus reducing the electron density (Prölss, 1995; Nakamura et al., 2009). This would lead to a negative ionospheric storm. On the other hand the mechanism of positive ionospheric storms cannot be explained by the N_2/O ratio mainly because when the ionospheric plasma moves to higher altitudes, resulting in reduced N_2 density, the recombination coefficient becomes low.

The following mechanism is assumed: ionospheric plasma rises to higher altitudes from an altitude of about 180 km where typically the production maximises, resulting in an increased F-layer electron density (Prölss, 1995; Nakamura et al., 2009). Although the mechanisms are broadly understood, an accurate prediction of positive and negative phases of ionospheric storms is difficult due to the absence of reliable observations in the upper atmosphere. Therefore, the development of empirical methods for prediction and estimation of ionospheric fluctuations are considered to have important practical and scientific significance.

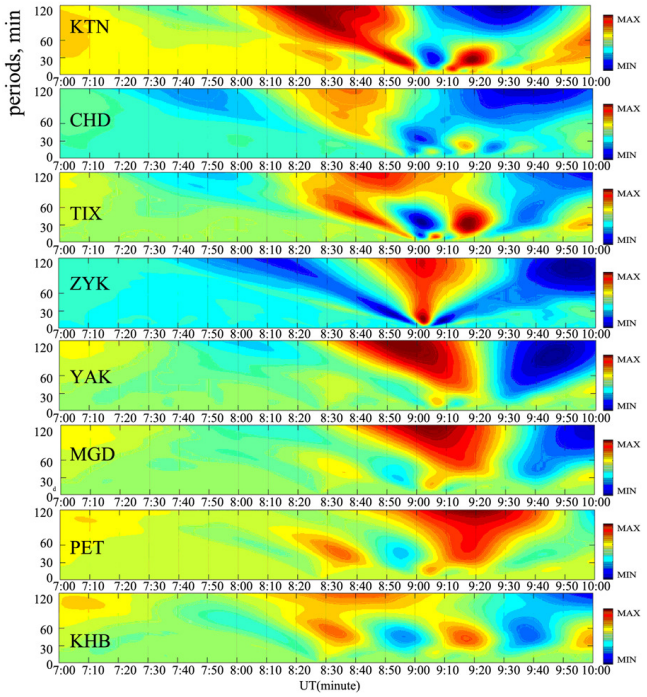

Figure 5. Estimation of a power of geomagnetic perturbations with 1-sec resolution in the interval of 07:00-10:00 UT on 5 April 2010 in color presentation. To show in detail a behavior of magnetic activity at middle latitudes the magnetic data from stations MGD and KHB were additionally used.

The results of processing of ionospheric data using author's method (see eqs. (4), (5)) for stations YAK and PET from 01 to 20 April 2010 are presented in Figure 6. Joint analysis of the data of these stations (Figure 6) shows a general behavior of the ionosphere. Intensity of the disturbances in the ionosphere increases substantially during periods of intense geomagnetic activity (see variations of K index). The strongest disturbances were observed on 6-8 April 2010. During the magnetic storm, the electron density in the F2 layer was significantly lower (more than 2.5 standard deviations from the background level in the interval marked by second and third dashed line in Figure 6) and a prolonged (~3 days) negative phase of the ionospheric storm was registered (shown in Figure 6 by blue color).

From Figure 6 a pre-storm enhancement in the electron density in the F2 layer on 4 April 2010 is seen as an abnormal (more than 1.5 standard deviations starting after first vertical dashed line from left) increase of the critical frequency foF2 relative to the background level (positive phase of ionospheric storm is shown in Figure 6 by red). The highest intensity of pre-storm ionospheric disturbances was observed at YAK (a peak after first vertical dashed line in third panel from top of Figure 6), the maximum of which coincides with the maximum at PET, where it occurred in about 6 hours before the beginning of the magnetic storm. Small-scale abnormal changes in the variations of ionospheric parameters during quiet and weak geomagnetic field conditions were also observed during the period from 1 April to 4 April 2010.

Results and Discussion

The analyzed magnetic event was observed on the Earth's surface at 08:26UT of April 5, 2010 and was identified as a magnetic storm with SSC. The speed of the solar wind during 07:22 to 08:03 UT had increased from 750 to 900 km/s. A globally observed intense substorm emerged 30 minutes later in the Earth's magnetosphere (Kleimenova et al., 2013). A substorm growth phase and localized dipolarization at 08:47 UT were followed by large dipolarizations at 09:03 and 09:08 UT, observed by GOES 11 in the midnight sector, and also by the three THEMIS spacecraft near X = −11, Y = −2 R_E (Connors et. al., 2011). Strong (THEMIS AL was less than -2000 nT) substorm interval was associated with the loss of communication with the Galaxy-15 satellite (Allen, 2010; Denig et al., 2010; Connors et al., 2011). During this substorm interval, localized and broad regions of ion energization were observed, demonstrating that magnetic reconnection and current disruption may have played a role during this very extreme event (Keesee et al., 2014).

Our results are in agreement with the above mentioned ones and most intense geomagnetic disturbances at stations in the far eastern region of Russia were observed in the interval of 08:34-09:34 UT due to SSC and substorm activity. The most intense geomagnetic disturbances during the event was observed at KTN (L~9) in the evening sector, but in the same interval, the strongest geomagnetic perturbations occurred at ZYK (L~4).

The geomagnetic activity associated with sporadic and continuous magnetic field reconnection under southward IMF component can last from days to a week and has been referred to as high-intensity long-duration continuous AE activity (HILDCAA) events (Tsurutani and Gonzalez, 1987). It is believed that some feature of these continuous (sporadic) plasma injections/HILDCAAs are the cause of the acceleration of magnetospheric energetic electrons to high energies.

For the analyzed event, IMF Bz remained negative during for ~1 day on 6 April 2010, except where it exhibited a northward peak (Figure 2). Figure 4 shows intense magnetic fluctuations at TIX and CHD (L~5-6) on 6 April 2010.

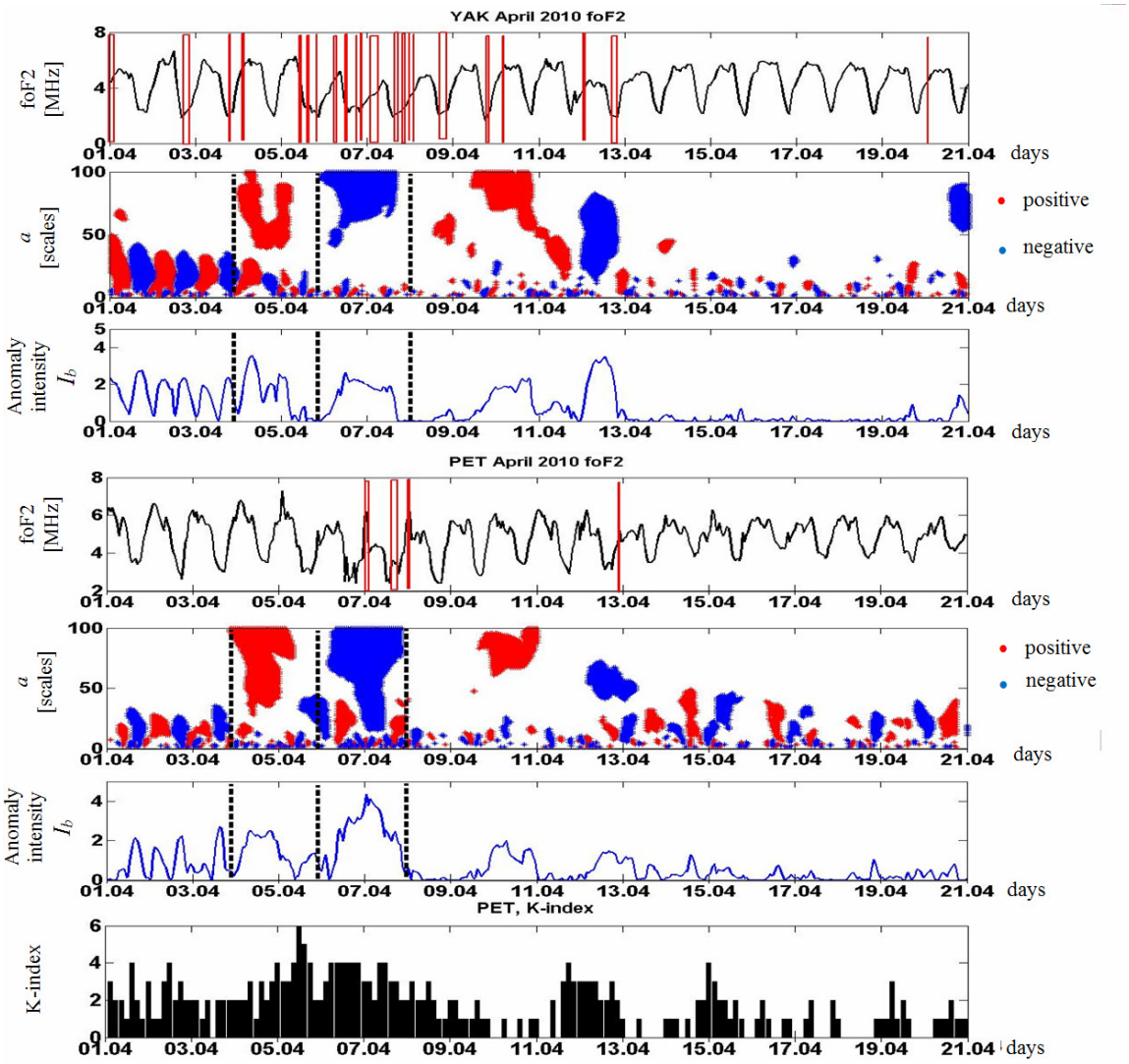

Figure 6: Variations of F2 layer critical frequency and results of wavelet analysis at YAK and PET, variations of geomagnetic K-index calculated using magnetic data at PET on 1-20 April 2010. For ionospheric stations YAK and PET are presented the highlighted anomalies (red - positive anomaly, blue - negative anomaly) and evaluation of wavelet power of ionospheric anomalies. Red rectangle marks the time interval filled by median values during data gap. The first vertical dashed line from left is moment of a pre-storm enhancement in the electron density in the F2 layer. Second and third dashed lines indicate interval of negative phase of the ionospheric storm.

Shimeis at al. (2012) have studied the ionospheric-magnetic disturbance during a strong magnetic storm on 5 April 2010 using GPS stations and MAGDAS station in Egypt. It is shown that at the beginning of the storm, an effect of the prompt penetration of the magnetosphere electric field was observed which strongly increased the TEC. During the recovery phase of the storm a signature of the ionospheric disturbance dynamo due to wind produced by Joule heating in the auroral zone was registered.

Fathy et al. (2014) continued an analysis of the magnetic storm on 5 April 2010 to separate the magnetic disturbance associated to the ionospheric disturbance dynamo (Ddyn) from the magnetic disturbance associated to the prompt penetration of magnetospheric electric field (DP2) using INTERMAGNET magnetometers along three longitudinal sectors: African-European, Asian, and American. It is found that, in the different longitude sectors, the responses of ionospheric disturbance dynamo had been different. On the first day, 5 April 2010, all INTERMAGNET stations exhibited similar and simultaneous signature of the prompt penetration of the magnetospheric convection electric field at the European-African sector. On 6-8 April 2010 the disturbance is different from one station to another station. This fact indicated that the disturbance is not due to prompt penetration of the convection electric field. The Ddyn disturbance reduces the amplitude of the daytime H component at low latitudes during the four consecutive days.

Our ionospheric data highlights the effect of the prompt penetration of the convection electric field which drastically decreased the foF2 values at YAK

and PET. On 6-7 April 2010 at YAK and PET, prolonged negative phase of the ionospheric storm (blue color in Figure 6) was observed. Such behavior of the ionosphere shown by the ground-based measurements, as well as total electron concentration (TEC) data, before and during the periods of strong and moderate magnetic storms is noted in (Buresova and Laštovička, 2007; Mansilla, 2007; Lui et al., 2008a,b; Nogueira et al., 2011; Saranya et al., 2011; Adekoya and Chukwuma, 2012; Danilov, 2013; Mandrikova et al., 2015). A significant relationship between the intensity of ionospheric anomalies and frequency of their occurrence, on the one hand, and of solar and geomagnetic activity on the other is shown for different regions in (Lui at al., 2008a,b; Nogueira et al., 2011; Saranya et al., 2011; Danilov, 2013; Mandrikova et al., 2014a, 2015).

Special attention in the recent researches (Kane, 2005; Buresova and Laštovička, 2007; Lui et al., 2008a, b; Danilov, 2013) have been paid pre-storm enhancements of critical frequency foF2 and TEC. Results (Kane, 2005; Lui at al., 2008a, b; Nogueira et al., 2011; Danilov, 2013; Mandrikova et al., 2015) are shown that pre-storm enhancements in the ionosphere can occur in the background of quiet and weakly disturbed geomagnetic field and their duration can range from a few hours to half a day. These results show that the effect is evident, but some questions about the nature and mechanisms remain still open. Analysis of the event on April 5, 2010 (Figure 6) confirm these effects and illustrates a common picture of the behavior of ionosphere over Russian Far East. The key question is, whether pre-storm ionospheric disturbances are linked with geomagnetic activity. The authors are of the opinion presented in the review by Danilov (2013), and believe that such ionospheric effects are associated with a certain channel of energy penetration from the interplanetary space and magnetosphere. In this case, pre-storm ionospheric disturbances may signal the forthcoming geomagnetic storm that has important applications (Adekoya and Chukwuma, 2012; Danilov, 2013).

The present results also demonstrate the effectiveness of the proposed computing solutions, which allowed us to highlight effects and perform a detailed analysis of the dynamics of the ionosphere during disturbed period in the presence of a large number of missing data (gaps associated with strong disturbances in the ionosphere and the limited capacity of the ionosondes).

Acknowledgments

This work was supported in part by JSPS Core-to-Core Program (B. Asia-Africa Science Platforms), Formation of Preliminary Center for Capacity Building for Space Weather Research and International Exchange Program of National Institute of Information and Communication Technology (NICT), the grant of the Russian Science Foundation № 14-11-00194 (MOV) and the Russian Foundation for Basic Research (grants 15-45-05090 (MAV), 15-45-05108 (BDG)).

References

Adekoya B.J., and Chukwuma V.U.: 2012, Indian Journal of Radio and Space Physics, 41(6), 606616.

Allen, J.: 2010, Space Weather, 8, S06008, doi:10.1029/2010SW000588.ax.

Baishev, D.G., Moiseyev, A.V., Boroyev, R.N., et al.: 2013, Science and education (in Russian), 1(63). 7-10.

Buonsanto, M.J.: 1999, Space Science Reviews, 88, 563-601.

Burešová, D., and Laštovička J.: 2007, Adv. Space Res., 39, 1298-1303.

Connors, M., Russell, C.T., and Angelopoulos V.: 2011, Ann. Geophys., 29, 619-622, doi:10.5194/angeo-29-619-2011.

Danilov, A.D.: 2001, J. Atmos. Sol. Terr. Phys., 63, 441-449.

Danilov, A.D.: 2013, Adv. Space Res., 52(3), 343-366.

Danilov, A.D., and Laštovička, J.: 2001, Int. J. Geomag. Aeron., 2, 209-224.

Denig, W.F., Green, J.C., Wilkinson D.C., et al.: 2010, American Geophysical Union, Fall Meeting 2010, abstract #SH31D-03.

Fathy, I., Amory-Mazaudier, C., Fathy, A., et al.: 2014, J. Geophys. Res., 119, 4120-4133, doi: 10.1002/2013JA019510.

Kane, R.P.: 2005, Ann. Geophys., 23, 2487-2499.

Keesee, A.M., Chen M.W., Scime E.E., Lui A.T.Y.: 2014, J. Geophys. Res., 119, 8274-8287, doi: 10.1002/2014JA020466.

Kleimenova, N.G., Zelinskii, N.R., Kozyreva, O.V., et al.: 2013, Geomagnetism and Aeronomy, 53, 313-320.

Lepping, R. P., et al.: 1995, Space Sci. Rev., 71, 207-229.

Liu, L., Wan, W., Zhang, M.-L., Zhao, B.: 2008a, Ann. Geophys., 26(4), 893-903.

Liu, L., Wan, W., Zhang, M.-L., Zhao, B., Ning, B.: 2008b, J. Geophys. Res., 113, A02311, doi:10.1029/2007JA012832.

Mandricova, O.V., Solovev, I.S., and Baishev, D.G.: 2014, Bulletin of Kamchatka State Technical University (in Russ.), 27, 8-13.

Mandrikova, O.V., Fetisova, N.V. (Glushkova, N.V.), Polozov, Y.A., Solovev, I.S., Kupriyanov, M.S.: 2015, Earth Planet. Space, 67, doi: 10.1186/s40623-015-0301-4.

Mandrikova, O.V., Glushkova, N.V., Zhivet'ev, I.V.: 2014a, Geomagnetism and Aeronomy, 54(5), 593-600, doi: 10.1134/S0016793214050107.

Mandrikova, O.V., Solovev, I.S, Zalyaev, T.L.: 2014b, Earth Planet. Space, 66, doi:10.1186/s40623-014-0148-0.

Mandrikova, O.V., Solovjev, I., Geppenerc, V., Taha Al-Kasasbehd, R., Klionskiy, D.: 2013, Dig. Signal Processing. 23, 329-339.

Mansilla, G.A.: 2007, Studia Geophysica et Geodaetica, 51(4), 563-574.

Levin, B.R.: 1963, Theoretical basis of statistical radio techniques. Fizmatgiz, Moscow (in Russian).

Mendillo, M.: 2006, Rev. Geophys., 44, RG4001, doi:10.1029/2005RG000193.

Möstl, C., Temmer, M., Rollett, T., et al: 2010, Geophys. Res. Lett., 37, L24103, doi:10.1029/2010GL045175.

Nakamura, M., Maruyama, T., Shidama Y.: 2009, Journal of the National Institute of Information and Communication Technology, 56, 391-406.

Nogueira, P.A.B., Abdu, M.A., Batista, I.S., de Siqueira, P.M.: 2011, J. Atmos. Sol. Terr. Phys., 73, 1535-1543.

Ogilvie, K. W., et al.: 1995, Space Sci. Rev., 71, 55-77.

Prolls, G.: 1995, in H. Volland (ed.), Handbook of Atmospheric Electrodynamics, Vol 2, CRC Press/ Boca Raton, 195-248.

Reinisch, B. W., Haines, D.M., Bibl, K., et al.: 1997, Radio Sci., 32(4), 1681–1694, doi:10.1029/97RS00841.

Rees, D.: 1995, J. Atmos. Terr. Phys., 57, 1433.

Saranya, P.L., Venkatesh, K., Prasad, D.S.V.V.D., Rama Rao, P.V.S., Niranjan, K.: 2011, Adv. Space Res., 48(2), 207-217.

Shimeis, A., Fathy, I., Amory-Mazaudier, C., et al.: 2012, J. Geophys. Res., 117, A07309, doi:10.1029/2012JA017753.

Tsurutani, B.T., and Gonzalez, W.D.: 1987, Planet. Space Sci., 35, 405, doi:10.1016/0032-0633(87) 90097-3.

Yumoto K. and the MAGDAS Group: 2006, in N. Gopalswamy and A. Bhattacharya (ed.), Solar Influence on the Heliosphere and Earth's Environment: Recent Progress and Prosp., 399-405.